



# Convective Stability of $CO_2$ Sequestration in a Porous Medium

M. H. DarAssi\*

*Department of Basic Sciences, Princess Sumaya University for Technology, Amman, Jordan.*

Received: September 9, 2020; Revised: March 22, 2021

**Abstract:** We considered an incompressible fluid-saturated porous layer bounded by two infinite parallel plates. The Boussinesq approximation and Darcy's law are applied. The permeability is assumed to be a linear function of the depth  $z$ . The linear stability is investigated. The long wavelength expansion method is applied to conduct the weakly nonlinear stability analysis. The evolution equation is derived and analyzed. A uniformly valid periodic solution of the evolution equation is obtained by the application of the Poincaré-Lindstedt method. Some numerical simulations are presented.

**Keywords:** *stability analysis; long wavelength method; Poincaré-Lindstedt method; periodic solution; carbon sequestration.*

**Mathematics Subject Classification (2010):** 76E20, 76E15, 76S05, 76-10, 76E06.

## 1 Introduction

The greenhouse effect of carbon dioxide is one of the most urgent problems that face the humanity. The greenhouse gas emissions can be reduced through the geological carbon dioxide sequestration in deep rock formations. Geological carbon dioxide sequestration is the process of trapping  $CO_2$  that is produced by burning fossil fuels or any other chemical or biological processes and placing it in a deep rock formation (thousands of feet deep) for a long-term storage so that it will not affect the atmosphere. This process is comprised of three stages: capturing, transporting, and injecting  $CO_2$  into the geological formation such as gas reservoirs, unmineable coal seams, and basalt formations [1–4]. The capacity of such formations is estimated worldwide to be between 675–900 Gt of carbon in the gas reservoirs, between 1000–10000 Gt for saline aquifers, and for unmineable coal it

---

\* Corresponding author: <mailto:m.assi@psut.edu.jo>

is between 3-200 Gt of carbon. Depending on the geothermal gradient and the fluid properties,  $CO_2$  migrates and reacts with the rock formation. Hence, many trapping mechanisms such as structure trapping, residual-phase trapping, solubility trapping, and mineral trapping have been contributing to retention of the  $CO_2$  sequestration for a very long period [5].

In the past few decades, the interest in the understanding of the convection in porous media has been increased. Vast studies have been made in several branches of engineering and science [6–23]. Natural convection in porous media has been explored in numerous papers. Horton and Rogers in 1945 and Lapwood in 1948, carried out the stability analysis of the convection of a fluid in a porous medium for a horizontal fluid layer problem. The critical Rayleigh number was  $4\pi^2$  [6, 7]. Foster [8, 9] applied the amplification theory to study time dependent coefficients of a system of partial differential equations. They determined the onset of instability in terms of critical time. King et. al. use the amplification method to study the carbon dioxide sequestration problem in anisotropic porous media [10, 11]. The problem of convection of carbon dioxide storage in saline aquifers has been investigated by Hassanzadeh et. al. [12–14] and Emami-Meybodi et. al. [15, 16]. A step-function base profile has been considered by Wanstall and Hadji [17]. They conducted the stability analysis by applying the normal modes approach. They investigated the linear and nonlinear stability to obtain the minimum thickness of the layer of the saturated brine that is required for the fluid motion.

Neufeld et. al. [18] performed laboratory experiments to study the convective behavior of  $CO_2$  brine. Their numerical simulations depicted the relation between the convective flux and the Rayleigh number. To study the dissolution of  $CO_2$  into brine, Neufeld et. al. [19] used mixtures of methanol and ethylene-glycol solutions in water in their laboratory experiments. Batchelor and Nitsche [20] considered the small disturbance of a stationary stratified fluid. They showed numerically that the growth rate is a function of the Rayleigh number, the Prandtl number, and the horizontal wavenumber of the disturbance. A nonlinear stability analysis of a convection in porous layer with finite conducting boundaries has been conducted by Riahi [21]. Hill and Morad [22] have studied the convective stability in an anisotropic porous medium. They considered a water-saturated porous layer bounded by two horizontal parallel plates. The Darcy equation with variable permeability is used to govern the fluid motion.

Vo and Hadji [23] investigated the linear and weakly nonlinear stability of the convection induced by sequestration of  $CO_2$  in a perfectly impervious geological formation. They considered a horizontal layer of brine saturated porous medium confined between two horizontal planes that are impermeable to mass flow. They used the classical normal modes to investigate the linear stability. The weakly nonlinear stability is studied by applying the long wavelength asymptotic expansion method that is valid for small Damköhler numbers. They determined that the Rayleigh number and its corresponding wavenumber are independent of the depth of the formation.

Vo and Hadji [23] described the model that mimics the Rayleigh-Taylor instability to study the carbon sequestration. They considered the heavy carbon-saturated layer ( $Z_0$  1) on the top of the light free-carbon layer ( $0$   $Z_0$ ). This situation leads to a very thin unstable stratified layer at  $z = Z_0$  across which buoyancy diffuses. The stratified basic profile is defined as a step function and the reference carbon concentration in porous

media is defined by

$$C_{ref}(z) = \begin{cases} 0, & 0 < z < Z_0, \\ \frac{z - Z_0}{1 - Z_0}, & Z_0 < z < 1. \end{cases}$$

The basic temperature profile is defined by  $T_B = T_1 + (T_2 - T_1)\mathcal{H}(z - Z_0)$ , where  $T_1$  and  $T_2$  are temperature values at the lower region and the upper region, respectively, and  $\mathcal{H}$  is the Heaviside function.

In this paper, we considered the same model as that proposed by Hill and Morad [22], where the instability is quantified in terms of the long time evolution with the Dirichlet and Neumann boundary conditions at the upper and lower walls, respectively. This paper is organized as follows: In Section 2, a full description of the problem is presented and the problem is governed by a mathematical model. Moreover, the basic profile of the concentration is derived. In Section 3, the steady-state linear stability is studied. The weakly nonlinear stability is investigated by the application of the long wavelength expansion method in Section 4. In Section 5, the Poincaré-Lindstedt method is used to obtain a uniformly valid periodic solution. Numerical simulations are introduced and the results are concluded in Section 6.

## 2 Mathematical Formulation

In this section we considered the mathematical model that has been discussed by Hill and Morad [22], Wanstall and Hadji [17], and Vo and Hadji [23]. That is, we considered an incompressible fluid-saturated porous layer bounded by two infinite horizontal parallel plates. We assumed that the Boussinesq approximation and Darcy’s law are applied and the fluid motion is governed by the Darcy equation. Therefore, the nondimensionalized governing system of equations comprised of the Darcy equation, the continuity equation, the conservation of carbon dioxide equation, and the equation of solute balance is given by

$$\nabla \cdot \mathbf{u} = 0, \tag{1a}$$

$$\frac{1}{\mathcal{F}(z)} \mathbf{u} = \nabla p - c \mathbf{k}, \tag{1b}$$

$$\frac{\partial c}{\partial \hat{t}} + \mathbf{u} \cdot \nabla c + \left( \frac{dM(z)}{dz} \right) w = \frac{\xi}{R} \nabla_H^2 c + \frac{1}{R} \left( \frac{\partial^2 c}{\partial z^2} - Da c \right), \tag{1c}$$

$$\rho = \rho_0 [1 + \gamma_c (c - C_0)], \tag{1d}$$

where  $M(z)$  is the basic profile of concentration,  $p$  is the pressure,  $\mathbf{k}$  is the vertical unit vector,  $\rho_0$  is the reference density,  $\xi = \frac{\kappa_h}{\kappa_v}$  is the ratio of the horizontal and vertical

solal difusion,  $\mathcal{F}(z)$  is the  $z$ -dependent dimensionless permeability,  $Da = \frac{\beta H^2}{\psi_p \kappa_v}$  is

the Damökhler number,  $\beta$  is the reaction rate and the control parameter, namely, the

Rayleigh-Darcy number  $R = \frac{\gamma_c g H K_0 C_0}{\phi_p \nu \kappa_v}$ , where  $\gamma_c$  is the solal expansion,  $g$  is the

gravitational constant,  $H$  is the distance between the two plates,  $K_0$  is the reference permeability value,  $C_0$  is the reference concentration of  $CO_2$ ,  $\phi_p$  is the porosity,  $\nu$  is the kinematic viscosity, and  $\kappa_v$  is the vertical  $CO_2$  diffusion coefficient. The system is subject to the following boundary conditions:

$$\mathbf{u} = \mathbf{0}, \quad \text{at } z = 0, z = 1,$$

and

$$\frac{\partial c}{\partial z} = 0, \quad \text{at } z = 0, z = 1.$$

For more details about this model, please, refer to [22], [17] and [23]. Figure 1 describes the problem with its boundary conditions.

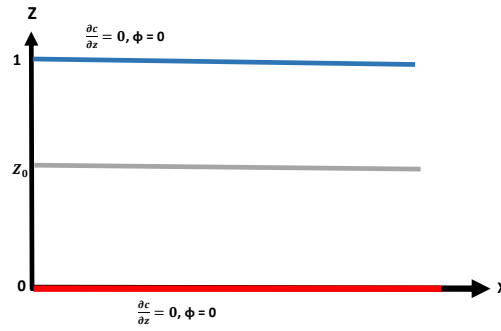


**Figure 1:** An incompressible fluid-saturated porous layer bounded by two infinite horizontal parallel plates.

The step function base state is modeled by the partial differential equation

$$\frac{\partial C_B}{\partial t} = \frac{1}{R} \left( \frac{\partial^2 C_B}{\partial z^2} - Da C_B \right), \quad 0 \leq z \leq 1, \quad t > 0, \quad (2)$$

subject to the boundary conditions

$$\frac{\partial C_B}{\partial z} = 0 \quad \text{at } z = 0, \quad z = 1,$$

and the initial condition

$$C_B(z, 0) = \begin{cases} 0, & 0 \leq z < Z_0, \\ 1, & Z_0 \leq z \leq 1. \end{cases}$$

The solution of equation (2) is given by

$$C_B(z, \hat{t}) = 1 - Z_0 - 2 \sum_{n=1}^{\infty} \frac{\sin(n\pi Z_0)}{n\pi} \cos(n\pi z) \exp\left(-\frac{Da + n^2 \pi^2}{R} \hat{t}\right). \quad (3)$$

Figure 2 below shows the plot of the concentration basic profile as a function of  $z$  for some values of  $t$ .

Following [17], the basic concentration profile consists of a light layer  $0 < z < Z_0$  under a heavier one,  $Z_0 < z < 1$ , which can be described by the Heaviside function, i.e.,

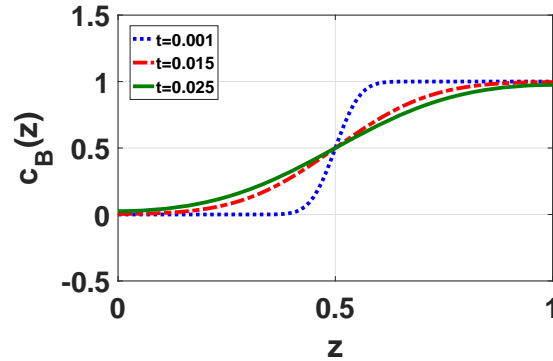


**Figure 2:** The plot of the concentration profile  $c_B(z)$  as a function of the depth of the fluid layer  $z$  and  $t = 0.001$  (dotted line),  $t = 0.015$  (dashed line) and  $t = 0.025$  (solid line).

$M(z) = \mathcal{H}(z - Z_0)$ . Upon subtracting the basic state profiles, introducing the poloidal representation for the velocity field  $\mathbf{u} = \nabla \times (\nabla \times \phi \mathbf{k})$ , and considering the vertical component of the velocity, we removed the pressure term and the system of equations (1a)-(1d) reduced to

$$\mathcal{F}(z)\nabla^2\phi - \mathcal{F}'(z)\frac{d\phi}{dz} = -\mathcal{F}^2(z)c, \tag{4a}$$

$$c_t + (\nabla_H\phi_z) \cdot (\nabla_H c) - \nabla_H^2\phi c_z = -\nabla_H^2\phi\delta(z - Z_0) + \frac{\xi}{R}\nabla_H^2c + \frac{1}{R}\left(\frac{\partial^2c}{\partial z^2} - Da c\right), \tag{4b}$$

where  $\phi$  is the poloidal representation for the divergence velocity field,  $\delta(z - Z_0)$  is the Dirac delta function,  $c$  is the deviation of the concentration in volume fraction from the diffusive state,  $R$  is the Rayleigh-Decay number, and  $\nabla_H = (\partial/\partial x, \partial/\partial y)$ . It is subject to the following boundary conditions:

$$\phi = 0 \text{ at } z = 0, 1, \text{ and } \frac{\partial c}{\partial z} = 0 \text{ at } z = 0, z = 1. \tag{5}$$

Upon introducing the transformation  $\Phi = R\phi$  and  $\frac{\partial}{\partial t} = R\frac{\partial}{\partial \hat{t}}$ , the equations (4a) and (4b) reduced to

$$\mathcal{F}(z)\nabla^2\Phi - \mathcal{F}'(z)\frac{d\Phi}{dz} = -R\mathcal{F}^2(z)c, \tag{6a}$$

$$c_t + (\nabla_H\Phi_z) \cdot (\nabla_H c) - \nabla_H^2\Phi c_z = -\nabla_H^2\Phi\delta(z - Z_0) + \xi\nabla_H^2c + \left(\frac{\partial^2c}{\partial z^2} - Da c\right) \tag{6b}$$

subject to the following boundary conditions:

$$\Phi = 0 \text{ at } z = 0, 1, \text{ and } \frac{\partial c}{\partial z} = 0 \text{ at } z = 0, z = 1. \tag{7}$$

To investigate the linear and weakly nonlinear stability, we will assume  $\xi = 1$ , the convection effect dominates over the reaction effect, i.e.,  $Da = 0$  and  $\mathcal{F}(z) = 1 + \lambda z$ ,  $|\lambda| < 1$ , see [22]. Hence, equations (6a) and (6b) become

$$(1 + \lambda z)\nabla^2\Phi - \lambda\frac{d\Phi}{dz} = -R(1 + \lambda z)^2c, \tag{8a}$$

$$c_t + (\nabla_H \Phi_z) \cdot (\nabla_H c) - \nabla_H^2 \Phi c_z = -\nabla_H^2 \Phi \delta(z - Z_0) + \nabla_H^2 c + \frac{\partial^2 c}{\partial z^2} \quad (8b)$$

subject to the following boundary conditions:

$$\Phi = 0 \text{ at } z = 0, 1, \text{ and } \frac{\partial c}{\partial z} = 0 \text{ at } z = 0, z = 1. \quad (9)$$

### 3 Steady-State Linear Stability Analysis

Following the standard procedure used in [24], we obtained the following linearized system of equations governing the convective perturbations:

$$(1 + \lambda z) \nabla^2 \phi - \lambda \frac{d\Phi}{dz} = -(1 + \lambda z)^2 R c, \quad (10a)$$

$$\nabla^2 c = -\nabla_H^2 \phi \delta(z - Z_0) \quad (10b)$$

subject to the following boundary conditions:

$$\Phi = 0 \text{ at } z = 0, 1, \text{ and } \frac{\partial c}{\partial z} = 0 \text{ at } z = 0, z = 1. \quad (11)$$

To investigate the linear stability, we will introduce the normal modes

$$\Phi = e^{i\alpha \cdot \mathbf{x}} W(z), \quad c = e^{i\alpha \cdot \mathbf{x}} S(z), \quad (12)$$

where  $\mathbf{x} = (x, y)$  and  $|\alpha| = \alpha$ , we obtained

$$(1 + \lambda z)(D^2 W(z) - \alpha^2 W(z)) = -(1 + \lambda z)^2 R S(z), \quad (13a)$$

$$(D^2 - \alpha^2) S(z) = \alpha^2 W(z) \delta(z - Z_0), \quad (13b)$$

where  $D = \frac{d}{dz}$ . The corresponding Dirichlet and Neumann boundary conditions are  $W = 0$  at  $z = 0, 1$ ,  $DS = 0$  at  $z = 0, 1$ .

Expand  $W, S$  and  $R$  in terms of the small wave number  $\alpha$  and keep  $\lambda$  of order 1.  $W = W_0 + \alpha^2 W_2 + \dots$ ,  $S = S_0 + \alpha^2 S_2 + \dots$  and  $R = R_0 + \alpha^2 R_2$ . The  $O(1)$  problem is given by

$$D \left[ \frac{1}{1 + \lambda z} DW_0 \right] = -R_0 S_0, \quad (14a)$$

$$D^2 S_0 = 0 \quad (14b)$$

subject to the boundary conditions  $W_0(0) = W_0(1) = 0$  and  $DS_0(0) = DS_0(1) = 0$ . The solution of the equations (14a) and (14b) is given by

$$S_0 = 1,$$

$$W_0 = -\frac{R_0 G}{6} [(3z^2 + 2\lambda z^3) - L_1(2z + \lambda z^2)],$$

where  $L_1 = ((3/2) + \lambda)(1 - \lambda/2)$ .

When proceeding to the next order  $O(\alpha^2)$ , the equation of the concentration becomes

$$D^2 S_2 - S_0 = W_0 \delta(z - Z_0). \quad (15)$$

It has a unique solution if and only if the following condition is satisfied:

$$\int_0^1 S_0^* [S_0 + W_0 \delta(z - Z_0)] dz = 0,$$

where  $S_0^*$  is the solution of the adjoint problem of equation (14b), namely,  $D^2 S_0^* = 0$  with the corresponding boundary conditions  $DS_0^*(0) = DS_0^*(1) = 0$  to get  $S_0^* = 1$ . Upon applying the Fredholm alternative at  $O(\alpha^2)$  we obtain the critical Rayleigh-Darcy number

$$R_0 = \frac{6}{L_1(2Z_0 + \lambda Z_0^2) - (3Z_0^2 + 2\lambda Z_0^3)}.$$

As  $\lambda \rightarrow 0$ , the critical Rayleigh-Darcy number becomes  $R_0 = \frac{2}{Z_0 - Z_0^2}$ , which is consistent with what has been obtained in [17]. Figure 3 depicts that the plot of the critical Rayleigh-Darcy number  $R_0$  is decreased as the values of  $\lambda$  have increased in the right figure and the left figure shows that the minimum value of the critical Rayleigh-Darcy number  $R_0$  is at  $Z_0 = 0.5$  and it goes to infinity as  $Z_0$  approaches 0 or 1.

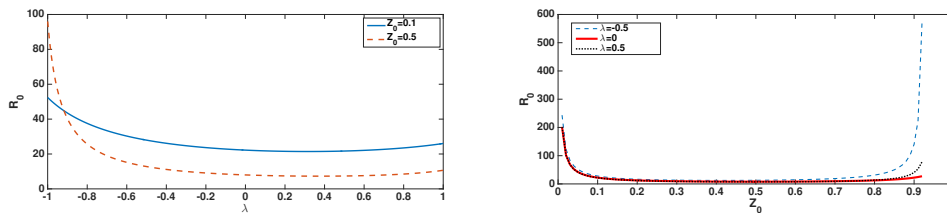


**Figure 3:** (Right) Plot of the critical Rayleigh-Darcy number  $R_0$  as a function of  $\lambda$  for  $Z_0 = 0.1$  (solid line) and  $Z_0 = 0.5$  (dashed line). (Left) Plot of the critical Rayleigh-Darcy number  $R_0$  as a function of  $Z_0$  for  $\lambda = 0$  (solid line),  $\lambda = -0.5$  (dashed line) and  $\lambda = 0.5$  (dotted line).

### 4 Weakly Nonlinear Stability

In this section we will investigate the weakly nonlinear stability by deriving the evolution equation. Following the long wavelength analysis procedure used in [25] and [26] we introduce the small parameter  $\epsilon \ll 1$  and we scale  $X = \epsilon x$ ,  $Z = z$ ,  $\tau = \epsilon^4 t$  and keep  $\lambda$  of  $O(1)$  quantity in equations (8a) and (8b). Moreover, we expand

$$\Phi = \Phi_0 + \epsilon^2 \Phi_2 + \dots, \quad c = c_0 + \epsilon^2 c_2 + \epsilon^4 c_4 + \dots$$

and  $R = R_0 + \epsilon^2 \hat{\mu}^2$ . The solution of the leading order problem that is described by

$$(1 + \lambda Z)D^2 \Phi_0 - \lambda D \Phi_0 = -(1 + \lambda Z)^2 R_0 c_0, \tag{16a}$$

$$D^2 c_0 = 0, \tag{16b}$$

with boundary conditions  $\Phi_0(0) = \Phi_0(1) = 0$  and  $Dc_0(0) = Dc_0(1) = 0$  is given by

$$\Phi_0 = -\frac{R_0 h}{6} [(3Z^2 + 2\lambda Z^3) - L_1 (2Z + \lambda Z^2)],$$

$$c_0 = h(X, \tau),$$

where  $L_1 = (1.5 + \lambda)(1 - \lambda/2)$ .

When proceeding to the next order, the  $O(\epsilon^2)$  problem is described by

$$D^2\Phi_2 - \lambda D\Phi_2 + (\Phi_0)_{XX} = -(1 + \lambda Z)[R_0 c_2 + \hat{\mu}^2 c_0], \quad (18a)$$

$$(D\Phi_0)_X (c_0)_X = -(\Phi_0)_{XX} \delta(Z - Z_0) + D^2 c_2 + (c_0)_{XX}. \quad (18b)$$

Application of the solvability condition to equation (18b) yields

$$R_0 = \frac{6 + 3\lambda}{(3 + 2\lambda)(Z_0 + (\lambda/2)Z_0^2) - (3Z_0^2 + 2\lambda Z_0^3)(1 + \lambda/2)}. \quad (19)$$

As  $\lambda \rightarrow 0$ , the critical Raleigh-Dracy number becomes  $R_0 = \frac{2}{Z_0 - Z_0^2}$ , which is consistent with what has been obtained in [17]. Proceeding to solve  $O(\epsilon^2)$  problem and because of the appearance of the  $\delta(Z - Z_0)$  term, we will divide the problem in two cases and equation (18b) will be divided into two equations:

$$\text{the light layer when } 0 < Z < Z_0: D^2 c_2^- = -R_0 (c_0)_X^2 (Z + \lambda Z^2) - (c_0)_{XX}, \quad (20a)$$

$$\text{the heavy layer when } 0 < Z < Z_0: D^2 c_2^+ = -R_0 (c_0)_X^2 (Z + \lambda Z^2) - (c_0)_{XX}, \quad (20b)$$

with boundary conditions  $Dc_2^-(0) = 0$  and  $Dc_2^+(1) = 0$ . Thus, the solutions of equations (20a) and (20b) are

$$c_2^- = -\frac{R_0 (h_X)^2}{36} [6Z^3 + 3\lambda Z^4 - L_1(3Z^2 + \lambda Z^3)] - \frac{h_{XX}}{2} Z^2 + A^-,$$

$$c_2^+ = -\frac{R_0 (h_X)^2}{36} [6Z^3 + 3\lambda Z^4 - L_1(3Z^2 + \lambda Z^3)] - \frac{h_{XX}}{2} (Z^2 - 2Z) + A^+,$$

where  $A^- = Z_0 h_{XX} + A^+$  and

$A^+ = \frac{R_0 (h_X)^2}{720} [(30 + 12\lambda) - 5L_1(4 + \lambda)] - \frac{h_{XX}}{6} (2 + 3Z_0^2)$ . Similarly, the solution of equation (18a) is given by

$$\begin{aligned} \Phi_2^- = & -\frac{R_0 h_{XX}}{10080} [92\lambda^3 Z^7 + (182 - 35L_1)\lambda^2 Z^6 - (588\lambda + 98\lambda^2 L_1) Z^5 \\ & - (840 + 140\lambda L_1) Z^4 + L_1 - ((1680 Z_0^2 - 3360 Z_0 + 1120)\lambda - 280 L_1) Z^3 \\ & - (2520 Z_0^2 - 5040 Z_0 + 1680) Z^2] + \frac{R_0^2 (h_X)^2}{30240} [72\lambda^2 Z^7 + (294\lambda - 35L_1) Z^6 \\ & + (252 - 210\lambda L_1) Z^5 - 210 L_1 Z^4 - (168\lambda^2) + 420\lambda - 70 L_1(4\lambda + \lambda^2)) Z^3 \\ & - (252\lambda + 630 - 105 L_1(4 + \lambda)) Z^2] - \frac{\hat{\mu}^2 h}{6} (2\lambda Z^3 + 3Z^2) + \frac{B^-}{2} (\lambda Z^2 + 2Z), \\ \Phi_2^+ = & -\frac{R_0 h_{XX}}{10080} [92\lambda^3 Z^7 + (182 - 35L_1)\lambda^2 Z^6 - (588\lambda + 98\lambda^2 L_1) Z^5 \\ & + (1260\lambda - 3360 - 70\lambda L_1) Z^4 - ((1680 Z_0^2 + 1120)\lambda - 1680 - 280 L_1) Z^3 \\ & - (2520 Z_0^2 + 1680) Z^2] + \frac{R_0^2 (h_X)^2}{30240} [72\lambda^2 Z^7 + (294\lambda - 35L_1) Z^6 + (252 - 210\lambda L_1) Z^5 \end{aligned}$$

$$-210 L_1 Z^4 - (168 \lambda^2) + 420 \lambda - 70 L_1(4\lambda + \lambda^2)) Z^3 - (252\lambda + 630 - 105 L_1 (4 + \lambda)) Z^2] \\ - \frac{\hat{\mu}^2 h}{6} (2\lambda Z^3 + 3 Z^2) + \frac{B^+}{2} (\lambda Z^2 + 2 Z) + A^{++},$$

where

$$B^+ = \frac{R_0 h_{XX}}{15120(2 + \lambda)} [288\lambda^3 - 546\lambda^2 - (1260 Z_0^4 + 5040 Z_0^2 + 1344)\lambda + 5040 Z_0^3 \\ + 7560 Z_0^2 + 2520 - L_1(105\lambda^3 + 294\lambda^2 - 420\lambda - 840)] \\ + \frac{R_0^2 (h_X)^2}{15120(2 + \lambda)} [(96\lambda^2 + 378\lambda - 378 - L_1 (35\lambda^2 + 175\lambda + 210))] + \frac{L_1 \hat{\mu}^2 h}{3},$$

$$B^- = \frac{Z_0^2 R_0 h_{XX}}{2} + B^+$$

$$A^{++} = \frac{R_0 h_{XX}}{10080} [96\lambda^3 + 182\lambda^2 - (1680 Z_0^2 + 448)\lambda + (840 - 1260\lambda) - 2520 Z_0^2 - 840 \\ - L_1(35\lambda^3 + 98\lambda^2 - 140\lambda - 280)] + \frac{R_0^2 (h_X)^2}{30240} [(96\lambda^2 + 378\lambda + 378 \\ - L_1 (35\lambda^2 + 175\lambda + 210))] + \frac{\hat{\mu}^2 h}{6} (2\lambda + 3) - \frac{B^+}{2} (2 + \lambda).$$

Proceeding to the next order  $O(\epsilon^4)$ , we have

$$D^2 c_4 = h_\tau + h_X (D\Phi_2)_X - (\Phi_0)_{XX} Dc_2 + (D\Phi_0)_X (c_2)_X + (\Phi_2)_{XX} \delta(Z - Z_0) - (c_2)_{XX} \tag{22}$$

with boundary conditions  $Dc_4(0) = Dc_4(1) = 0$ . Integrating equation (22) with respect to  $Z$  from  $Z = 0$  to  $Z = 1$ , yields the sought evolution equation

$$h_\tau = -\mathcal{A} h_{XXXX} - \hat{\mu}^2 \mathcal{B} h_{XX} + \mathcal{C} (h_X)_{XX}^2 + \mathcal{E} h_X^2 h_{XX}, \tag{23}$$

where

$$\mathcal{A} = -\frac{R_0 (Z_0 - Z_0^2)}{10080(2 + \lambda)} \{ [35(Z_0^4 + Z_0^3 + Z_0^2 + Z_0) L_1 - 96(Z_0^5 + Z_0^4 + Z_0^3 + Z_0^2 + Z_0)] \lambda^4 \\ + [(70Z_0^4 + 168Z_0^3 + 168Z_0^2 + 168Z_0 + 70) L_1 - (192Z_0^5 + 374Z_0^4 + 374Z_0^3 + 374Z_0^2 \\ + 374Z_0 + 192)] \lambda^3 + [(196Z_0^3 + 56Z_0^2 + 56Z_0 + 196) L_1 - (784Z_0^4 - 1484Z_0^2 - 84Z_0 \\ + 364)] \lambda^2 - [280(Z_0^2 + 2Z_0 + 1) L_1 - 56(36Z_0^3 + 21Z_0^2 + Z_0 + 16)] \lambda - 560(Z_0 + 1) L_1 \\ - 1680(2Z_0^2 - Z_0 + 1) \},$$

$$\mathcal{B} = \frac{1}{3} (Z_0 - Z_0^2) (\lambda Z_0 + L_1),$$

$$\mathcal{C} = \frac{R_0^2 (Z_0 - Z_0^2)}{30240(2 + \lambda)} \{ [(72Z_0^5 + 72Z_0^4 + 72Z_0^3 + 72Z_0^2 - 96Z_0) - 35(Z_0^4 + Z_0^3 + Z_0^2 \\ + Z_0) L_1] \lambda^3 + [(144Z_0^5 + 438Z_0^4 + 438Z_0^3 + 438Z_0^2 - 318Z_0 - 192) - (70Z_0^4 + 280Z_0^3 \\ + 280Z_0^2 - 140Z_0 - 70) L_1] \lambda^2 + [(588Z_0^4 + 840Z_0^3 + 840Z_0^2 - 756) - (420Z_0^3 + 630Z_0^2 \\ + 70Z_0 - 350) L_1] \lambda + 504Z_0^3 + 504Z_0^2 + 504Z_0 - 756 - 420(Z_0^2 + Z_0 - 1) L_1 \},$$

$$\mathcal{E} = \frac{R_0^2}{30240} [96\lambda^2 + 504\lambda + 756 - (84\lambda^2 + 476\lambda + 870)L_1 + (21\lambda^2 + 140\lambda + 280)L_1^2].$$

The evolution equation (23) is of parabolic type which is well-posed whenever the coefficient of the fourth derivative,  $-\mathcal{A}$ , is negative. Figure 4 shows that  $-\mathcal{A}$  is negative for all values of  $\lambda$  and  $Z_0$ .

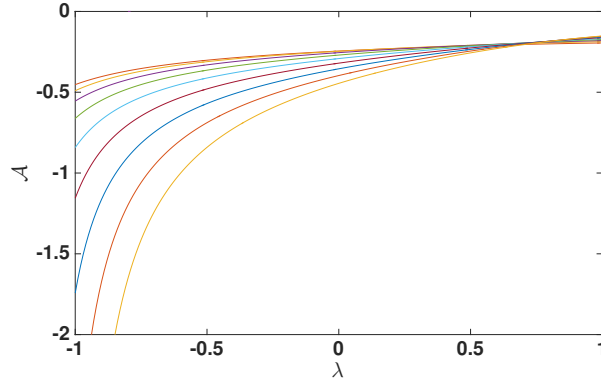


**Figure 4:** The plot of  $\mathcal{A}$  as a function of  $\lambda$ , where  $|\lambda| < 1$  and  $0 \leq Z_0 \leq 1$ .

## 5 Uniformly Valid Periodic Solution

Upon using the general procedure of the Biot number [27], the term  $-\hat{\gamma}h$  will be added to equation (23) to obtain

$$h_\tau = -\mathcal{A}h_{XXXX} - \hat{\mu}^2\mathcal{B}h_{XX} - \hat{\gamma}h + \mathcal{C}(h_X)_{XX}^2 + \mathcal{E}h_X^2 h_{XX}. \quad (24)$$

Upon introducing the following scales and transformations:  $h = af$ ,  $\xi = bX$ ,  $\tau = e\hat{\tau}$ ,  $\gamma = a\hat{\gamma}$  and  $e = 1/a$ , we have

$$f_\tau = -f_{\xi\xi\xi\xi} - 2\mu^2 f_{\xi\xi} - \gamma f + \Gamma(f_\xi)_{\xi\xi}^2 + (f_\xi)^2 f_{\xi\xi}, \quad (25)$$

where

$$a = \sqrt{\frac{\mathcal{A}}{\mathcal{E}}}, \quad b = \left(\frac{1}{\mathcal{A}}\sqrt{\frac{\mathcal{E}}{\mathcal{A}}}\right)^{1/4}, \quad \Gamma = \frac{\mathcal{C}}{\sqrt{\mathcal{A}\mathcal{E}}} \quad \text{and} \quad \mu^2 = \frac{\hat{\mu}^2 a b^2}{2}.$$

To investigate the stability of the static solution of equation (25) we consider the linear part

$$f_\tau = -f_{\xi\xi\xi\xi} - 2\mu^2 f_{\xi\xi} - \gamma f. \quad (26)$$

By introducing the normal modes  $f(\xi, \tau) = e^{\sigma\tau + i\theta\xi}$ , the following dispersion relation is obtained:

$$\sigma = -(\theta^2 - \mu^2) + \mu^4 - \gamma. \quad (27)$$

Therefore, the trivial static solution,  $f = 0$ , is unstable when  $\gamma < \mu^4$ . Upon introducing the small parameter  $\epsilon \ll 1$ , the weakly nonlinear stability of the evolution equation can

be investigated. To conduct the perturbation analysis around the linear solution, we expand

$$\gamma = \mu^4 - \epsilon \gamma_1 - \epsilon^2 \gamma_2, \quad \tau = \epsilon^2 \eta$$

and

$$f = \epsilon f_1 + \epsilon^2 f_2 + \epsilon^3 f_3 + \dots$$

The  $O(\epsilon)$  problem of equation (25) is described by

$$(f_1)_{\xi\xi\xi\xi} + 2\mu^2 (f_1)_{\xi\xi} + \gamma f_1 = 0 \tag{28}$$

whose period solution on the interval  $\left(\frac{-\pi}{\mu}, \frac{\pi}{\mu}\right)$  is  $f_1 = \cos(\mu\xi)$ . Because of the secular terms that are expected due to the linear part and the nonlinear terms, we will apply the Poincaré-Lindstedt method [28] to obtain a uniformly valid periodic solution. Substituting  $\nu = \omega\xi$  and expanding  $\omega = 1 + \epsilon\omega_1 + \epsilon^2\omega_2 + \dots$  in equation (25) we obtain

$$\omega^4 f_{\nu\nu\nu\nu} + 2\mu^2 \omega^2 f_{\nu\nu} + \gamma f = \omega^4 [\Gamma (f_\nu)_{\nu\nu}^2 + (f_\nu)^2 f_{\nu\nu}]. \tag{29}$$

Define the operator  $\mathcal{L}(f) = f_{\nu\nu\nu\nu} + 2\mu^2 f_{\nu\nu} + \mu^4 f$ . The leading order problem is described by

$$\mathcal{L}(f_1) = (f_1)_{\nu\nu\nu\nu} + 2\mu^2 (f_1)_{\nu\nu} + \mu^4 f_1 = 0 \tag{30}$$

whose solution is  $f_1 = \cos(\mu\nu)$ . The  $O(\epsilon^2)$  problem is described by

$$\mathcal{L}(f_2) = \gamma_1 \cos(\mu\nu) + \mu^4 \cos(2\mu\nu). \tag{31}$$

To remove the mixed-secular terms, we set  $\gamma_1 = 0$ , that is, there is no subcritical instability. Thus, the solution of  $\mathcal{L}(f_2) = \mu^4 \cos(2\mu\nu)$  is  $f_2 = \frac{1}{9} \cos(2\mu\nu)$ . When proceeding to the next order, the  $O(\epsilon^3)$  problem is described by

$$\begin{aligned} \mathcal{L}(f_3) = & \left[ \gamma_2 - 4\omega_1^2 \mu^4 - \frac{\Gamma \mu^4}{4} - \frac{5\mu^4}{9} \right] \cos(\mu\nu) - \frac{20\omega_1 \mu^4}{9} \cos(2\mu\nu) \\ & + \left[ \frac{\Gamma \mu^4}{4} + \frac{5\mu^4}{9} \right] \cos(3\mu\nu). \end{aligned} \tag{32}$$

To remove the secular term, we set  $\gamma_2 - 4\omega_1^2 \mu^4 - \frac{\Gamma \mu^4}{4} - \frac{5\mu^4}{9} = 0$  and then we solve for  $\omega_1$  to get

$$\omega_1 = \pm \sqrt{\frac{\gamma_2}{4\mu^4} - \frac{\Gamma}{16} - \frac{5}{36}}.$$

Therefore, the solution of equation (32) is given by

$$f_3 = -\frac{5\omega_1}{36} \cos(2\mu\nu) + \frac{9\Gamma + 20}{2916} \cos(3\mu\nu). \tag{33}$$

Thus, a uniformly valid steady state of equation (25) is given by

$$\begin{aligned} f = & \epsilon \cos((1 + \epsilon\omega_1)\xi\mu) + \epsilon^2 \frac{1}{9} \cos(2(1 + \epsilon\omega_1)\xi\mu) \\ & + \epsilon^3 \left[ -\frac{5\omega_1}{36} \cos(2(1 + \epsilon\omega_1)\xi\mu) + \frac{9\Gamma + 20}{2916} \cos(3(1 + \epsilon\omega_1)\xi\mu) \right]. \end{aligned} \tag{34}$$

Figure 5 shows the plot of the uniformly valid periodic solution of equation (25) as a function of  $\xi$  for  $\gamma_2 = 10$  and  $\mu = 0.7$ .

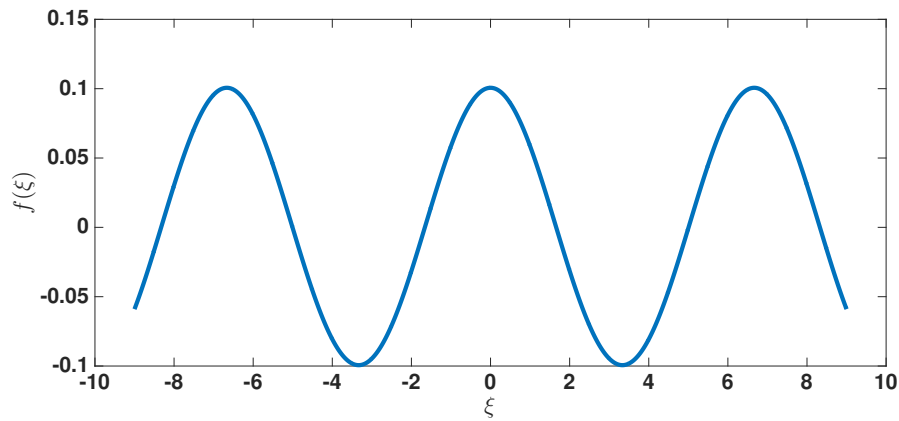


**Figure 5:** A plot of the periodic solution of equation (25) as a function of  $\xi$  with  $\gamma_2 = 10$  and  $\mu = 0.7$ .

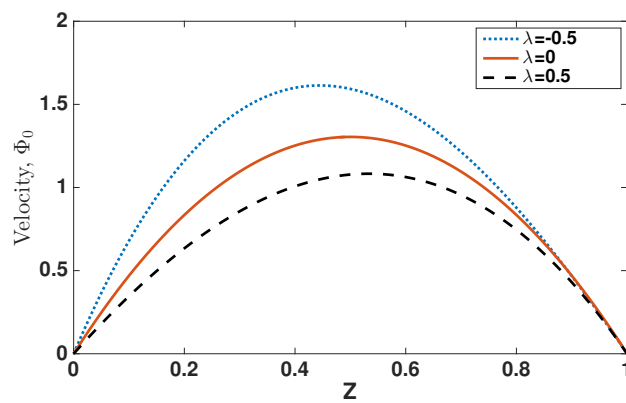


**Figure 6:** The plot of the velocity  $\Phi_0$  as a function of the depth  $Z$  with  $\lambda = -0.5$  (dotted line),  $\lambda = 0$  (solid line) and  $\lambda = 0.5$  (dashed line).

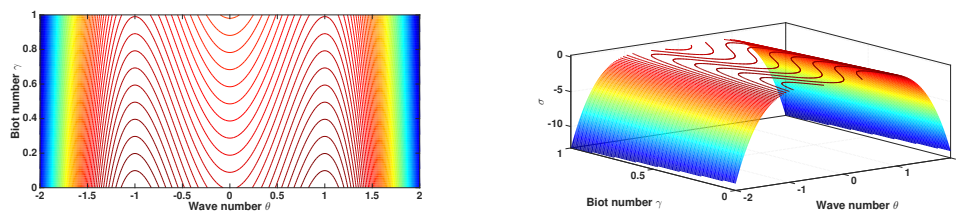


**Figure 7:** The 2D plot of the growth rate  $\sigma$  as a function of the wave number  $\theta$  and the Biot number  $\gamma$  (left figure) and the 3D plot (right figure) with  $\mu = 0.7$ .

## 6 Discussion and Conclusion

In this paper, we studied the mathematical model that was proposed by Hill and Morad [22]. That is, we considered an incompressible fluid-saturated porous layer bounded by two infinite parallel plates. The Boussinesq approximation and Darcy's law are applied. The permeability is assumed to be a linear function of the depth  $z$ , namely,  $\mathcal{F}(z) = 1 + \lambda z$ . The base state of the model consists of a light free-carbon layer,  $[0, Z_0)$ , at the bottom and a heavier carbon-saturated layer,  $(Z_0, 1]$ , at the top, Figures 1 and 2 illustrate the problem. Steady-state linear stability analysis is conducted and the critical Rayleigh-Darcy number is obtained, namely,  $R_0 = \frac{6}{L_1(2Z_0 + \lambda Z_0^2) - (3z^2 + 2\lambda Z_0^3)}$ . If we let  $\lambda \rightarrow 0$ , then the

critical Rayleigh-Darcy number becomes  $R_0 = \frac{2}{Z_0 - Z_0^2}$ , which is consistent with the value obtained in [17]. The relation between the critical Rayleigh-Darcy number and the permeability coefficient  $\lambda$  is depicted in Figure 3.

The weakly nonlinear stability analysis is conducted by the long wavelength expansion method and the evolution equation (23) is derived and analyzed. Figure 6 shows the velocity,  $\Phi_0$ , as a function of the depth  $Z$  for different values of the permeability coefficient  $\lambda$ .

Moreover, the dispersion equation is obtained and the relation between the growth rate, the Biot number and the wave number is depicted in Figure 7 and a uniformly valid periodic solution is obtained by the application of the Poincaré-Lindstedt method. The plot of this periodic solution is shown in Figure 5.

## References

- [1] R. Sedjo and B. Sohngen. Carbon Sequestration in Forests and Soils. *Annual Reviews* **4** (2012) 127–144.
- [2] S. Bachu. Sequestration of  $CO_2$  in geological media in response to climate change: road map for site selection using the transform of the geological space into the  $CO_2$  phase space. *Energy Convers Mgmt.* **43** (2002) 87–102.
- [3] S. Bachu. Sequestration of  $CO_2$  in geological media: criteria and approach for site selection in response to climate change. *Energy Convers Mgmt.* **41** (2000) 953–970.
- [4] U.S. Department of Energy. Carbon Sequestration Key R&D Programs and Initiatives. <https://www.energy.gov/fe/science-innovation/carbon-capture-and-storage-research>.
- [5] International Panel on Climate Change. Carbon Dioxide Capture and Storage. *Cambridge University Press*, 2005.
- [6] C. W. Horton and F. T. Rogers. Convection currents in porous media. *J. Appl. Phys.* **16** (1945) 367–369.
- [7] E. R. Lapwood. Convection of a fluid in porous medium. *Proc. Cambridge Phil. Soc.* **44** (1948) 508–521.
- [8] T. Foster. Onset of convection in a layer of fluid cooled from above. *Phys. Fluids* **8** (1965) 1770–1774.
- [9] T. Foster. Onset of manifest convection in a layer of fluid with time-dependent surface temperature. *Phys. Fluids* **12** (1969) 2482–2487.
- [10] J. P. Ennis-King and L. Paterson. Role of convective mixing in the long-term storage of carbon dioxide in deep saline formulations. *Soc. Pet. Eng.* **10** (2005) 349–356.

- [11] J. P. Ennis-King, I. Preston and L. Paterson. Onset of convection in anisotropic porous media subject to a rapid change in boundary conditions. *Phys. Fluids* **17** 084107 (2005) 1–15.
- [12] H. Hassanzadeh, M. Poolladi-Darvish and D. W. Keith. Modelling of Convective Mixing in  $CO_2$  Storage. *J. Can. Petrol. Technol.* **44** (2005) 43–51.
- [13] H. Hassanzadeh, M. Poolladi-Darvish, and D. W. Keith. Stability of a fluid in a horizontal saturated porous layer: effect of non-linear concentration profile, initial, and boundary conditions. *Transp Porous Med.* **64** (2006) 193–211.
- [14] H. Hassanzadeh, M. Poolladi-Darvish, and D. W. Keith. Scaling Behavior of Convective Mixing, with Application to Geological Storage of  $CO_2$ . *AIChEJ* **53** (2007) 1121–1131.
- [15] H. Emami-Meybodi, H. Hassanzadeha, C. P. Greenb and J. Ennis-King. Convective dissolution of  $CO_2$  in saline aquifers: Progress in modeling and experiments. *International Journal of Greenhouse Gas Control* **40** (2015) 238–266.
- [16] H. Emami-Meybodi, H. Hassanzadeha, and J. Ennis-King.  $CO_2$  dissolution in the presence of background flow of deep saline aquifers. *Water Resources Research* **51** (2015) 2595–2615.
- [17] C. T. Wanstall and L. Hadji. A step function density profile model for the convective stability of  $CO_2$  geological sequestration. *J. Eng. Math.* **108** (2018) 53–71.
- [18] J. Neufeld, M. Hesse, A. Riaz, M. Hallworth, H. Techelepi, and H. Huppert. Convective dissolution of carbon dioxide in saline aquifers. *Geophysical Research Letters* **37** L22404 (2010).
- [19] J. Neufeld, D. Vella and H. Huppert. The effect of a fissure on storage in a porous medium. *J. Fluid Mech.* **639** (2009) 239–259.
- [20] G. Batchelor and J. Nitsche. Instability of stationary unbounded stratified fluid. *J. Fluid Mech.* **227** (1991) 357–391.
- [21] N. Riahi. Nonlinear convection in a porous layer with finite conducting boundaries. *J. Fluid Mech.* **129** (1983) 153–171.
- [22] A. Hill and M. Morad. Convective stability of carbon sequestration in anisotropic porous media. *Proceedings of the Royal Society A* **470** (2014) 2170.
- [23] L. Vo and L. Hadji. Weakly nonlinear convection induced by the sequestration of  $CO_2$  in a perfectly impervious geological formation. *Physics of Fluids* **29** 127101 (2017).
- [24] P. G. Drazin and W. H. Reid. *Hydrodynamic Stability*. Cambridge University Press: Cambridge, UK, 2004.
- [25] F. H. Busse and N. Riahi. Nonlinear thermal convection with poorly conducting boundaries. *J. Fluid Mech.* **96** (1980) 243–256.
- [26] C. J. Chapman and M. R. E. Proctor. Nonlinear Rayleigh-Bénard convection between poorly conducting boundaries. *J. Fluid Mech.* **101** (1980) 759–782.
- [27] M. R. E. Proctor. Planform selection by finite-amplitude thermal convection between poorly conducting slabs. *J. Fluid Mech.* **113** (1981) 469–485.
- [28] A. H. Nayfeh. *Introduction to Perturbation Techniques*. Wiley, New Yourk, 2004.